The origin and spread of locally adaptive seasonal camouflage in snowshoe hares

Matthew R. Jones[1,2], L. Scott Mills[3,4], Jeffrey D. Jensen[2], Jeffrey M. Good[1,3]

[1]Division of Biological Sciences, University of Montana, Missoula, MT 59812, USA.

[2]School of Life Sciences, Arizona State University, Tempe, AZ 85281, USA

[3]Wildlife Biology Program, University of Montana, Missoula, MT 59812, USA.

[4]Office of Research and Creative Scholarship, University of Montana, Missoula, MT 59812, USA.

Corresponding authors: matthew.r.jones.1@asu.edu, jeffrey.good@umontana.edu

Abstract

Adaptation is central to population persistence in the face of environmental change, yet we rarely precisely understand the origin and spread of adaptive variation in natural populations. Snowshoe hares (*Lepus americanus*) along the Pacific Northwest (PNW) coast have evolved brown winter camouflage through positive selection on recessive variation at the *Agouti* pigmentation gene introgressed from black-tailed jackrabbits (*L. californicus*). Here we combine new and published whole genome and exome sequences with targeted genotyping of *Agouti* in order to investigate the evolutionary history of local seasonal camouflage adaptation in the PNW. We find evidence of significantly elevated inbreeding and mutational load in coastal winter-brown hares, consistent with a recent range expansion into temperate coastal environments that incurred indirect fitness costs. The genome-wide distribution of introgression tract lengths supports a pulse of hybridization near the end of the last glacial maximum, which may have facilitated range expansion via introgression of winter-brown camouflage variation. However, signatures of a selective sweep at *Agouti* indicate a much more recent spread of winter-brown camouflage. Through simulations we show that the temporal lag between the hybrid origin and subsequent selective sweep of the recessive winter-brown allele can be largely attributed to the limits of natural selection imposed by simple allelic dominance. We argue that while hybridization during periods of environmental change may provide a critical reservoir of adaptive variation at range edges, the probability and pace of local adaptation will strongly depend on population demography and the genetic architecture of introgressed variation.

Introduction

Local adaptation is fundamental to the persistence of populations during periods of rapid environmental change. In particular, local adaption to marginal habitats may increase a species' niche breadth and range size (Holt and Gomulkiewicz 1997), enhancing their evolutionary resilience (Sgrò et al. 2011; Slatyer et al. 2013; Forsman 2016; Mills et al. 2018). Consequently, range edges where populations encounter marginal habitats and less favorable conditions may harbor crucial adaptive variation that facilitates long-term persistence in the face of environmental change (Hampe and Petit 2005; Hill et al. 2011; Cheng et al. 2014). Yet, range boundaries may also reflect the limits of natural selection if they are defined by environments where populations have failed to adapt (Antonovics 1976; Kirkpatrick and Barton 1997; Bridle and Vines 2007). Revealing how adaptive variation arises and spreads along range edges is, therefore, fundamental to understand the limitations of adaptation to new or changing environments (Ackerly 2003; Hampe and Petit 2005). However, we rarely possess detailed knowledge of the genetic basis and history of local adaptation in natural populations.

Several decades of theoretical research have established a framework for predicting demographic conditions along range margins, which are crucial in shaping population-level fitness and the potential for adaptation and range expansion. Populations inhabiting marginal habitats are generally predicted to be small and occur at low densities (Antonovics 1976; Kirkpatrick and Barton 1997), resulting in relatively reduced rates of beneficial mutation and levels of standing genetic variation (Pfennig et al. 2016). Small range-edge populations may further experience higher rates of inbreeding due to genetic drift (Wright 1931; Barton 2001) and accumulate deleterious variation (i.e., mutational load; Lynch et al. 1995; Willi et al. 2018), which can decrease the probability of population persistence (Mills and Smouse 1994). Elevated

52 individual inbreeding and mutational load along range edges may also reflect past histories of
53 adaptation and range expansion that result in non-equilibrium population dynamics. For instance,
54 mating between close relatives may increase in founder populations that have recently undergone
55 severe population contractions associated with range expansions (Frankham 1998). Likewise,
56 mutational load may be amplified through the colonization of new environments because
57 population contractions reduce the efficacy of selection against deleterious alleles at the
58 expansion front (i.e., expansion load; Peischl et al. 2013; Henn et al. 2016; González-Martínez et
59 al. 2017; Willi et al. 2018). Thus, when adaptation does occur along range margins it may
60 produce negative feedbacks on population fitness and evolutionary potential.
61 Patterns of migration into range edge populations are also pivotal to their fitness and
62 adaptive potential. Larger core populations are expected to produce relatively more migrants
63 than smaller edge populations, leading to asymmetric rates of gene flow between core and
64 peripheral habitats. In extreme scenarios, edge populations with low population growth rates
65 (λ<1) can be demographic sinks that are maintained by immigration from the core of the range
66 (Holt and Gomulkiewicz 1997; Griffin and Mills 2009). Highly asymmetric gene flow may
67 further reduce fitness and hinder adaptation along the range edge by continually swamping local
68 selection (Haldane 1930; Garcia-Ramos and Kirkpatrick 1997; Kirkpatrick and Barton 1997;
69 Kawecki 2008). However, gene flow from core populations into edge populations may ultimately
70 promote adaptive responses when edge populations are small and ecological gradients are
71 shallow (Polechová 2018; Bontrager and Angert 2019). Hybridization between species may also
72 facilitate adaptation and range expansion if edge populations intersect with the range of closely-
73 related species that are adapted to local habitats (Baker 1948; Lewontin and Birch 1966; Burke
74 and Arnold 2001; Rieseberg et al. 2007; Kawecki 2008; Pfennig et al. 2016). Introgression may

provide a crucial source of large-effect variation (Hedrick 2013), which is predicted to be scarce in small populations but often necessary for range-edge adaptation and expansion (Behrman and Kirkpatrick 2011; Gilbert and Whitlock 2016). Putative adaptive introgression has now been shown in numerous species (e.g., Song et al. 2011; Pardo-Diaz et al. 2012; Huerta-Sánchez et al. 2014; Lamichhaney et al. 2015; Miao et al. 2016; Jones et al. 2018; Oziolor et al. 2019) and has been specifically linked to range expansions in Australian fruit flies (Lewontin and Birch 1966), sunflowers (Rieseberg et al. 2007), and mosquitoes (Besansky et al. 2003). While hybridization may facilitate adaptation and range expansion via large-effect mutations (Hedrick 2013; Nelson et al. 2019), the factors influencing the pace of adaptive introgression are often unclear.

Snowshoe hares (*Lepus americanus*) are broadly distributed across boreal and montane forests of North America. Most populations of hares undergo seasonal molts between brown (summer) and white (winter) coats to maintain crypsis in snow-covered environments. Seasonal camouflage is a crucial component of fitness in this system (Mills et al. 2013) as hares that become mismatched with their environment experience dramatically increased predation rates (i.e., 3-7% increase in weekly survival mortality; Zimova et al. 2016). However, some hares have adapted to mild winter environments by remaining brown in the winter (Mills et al. 2018). Brown winter camouflage in snowshoe hares is relatively rare across the entire range (<5% of the range), but predominant along portions of the southern range edge in the Pacific Northwest (PNW; Nagorsen 1983) with occurrence closely tracking regions of low seasonal snow cover (Mills et al. 2018). As snow cover across North America continues to decline under climate change, it is predicted that winter-brown camouflage may spread from the edge to the interior of the range, enhancing the evolutionary resilience of snowshoe hares (Jones et al. 2018; Mills et al. 2018). We previously demonstrated that brown versus white winter camouflage in PNW

snowshoe hares is determined by a simple *cis*-regulatory polymorphism of the *Agouti* pigmentation gene that influences its expression during the autumn molt (Jones et al. 2018). The locally adaptive winter-brown allele is fully recessive and derived from introgressive hybridization with black-tailed jackrabbits (*Lepus californicus*), a closely-related scrub-grassland species that remains brown in the winter (Jones et al. 2018). Thus, the evolution of brown winter coats along coastal environments in the PNW represents one of the few verified cases of introgression underlying an adaptive trait of known ecological relevance in mammals (Taylor and Larson 2019).

The establishment of this genotype-to-phenotype link provides a powerful opportunity to examine how population history and hybridization shape local adaptation and expansion along the range edge. Here we seek to deepen our understanding of 1) the population history of PNW range edge snowshoe hares and 2) the origin and spread of winter-brown camouflage across coastal PNW environments. We first use previously published targeted exome data (61.7 Mb for 80 individuals; Jones et al. 2018) to estimate historical changes in population size (N), individual inbreeding coefficients, and mutational load in PNW hares. We then combine 11 whole genome sequences (WGS; six new and five previously published) with 61 newly assembled complete mitochondrial genomes and targeted genotyping of the introgressed *Agouti* region across 106 hares to resolve the timing of hybridization with black-tailed jackrabbits and the subsequent spread of winter-brown coat color variation. We use these data to test theoretical predictions for the maintenance and spread of adaptive variation in peripheral environments. Our study provides rare empirical insight into the dynamic interplay of environmental change, hybridization, and selection along range-edge environments and its evolutionary consequences.

Methods

Genomic data generation

All sample collection with live animals was performed under approved state permits and associated Animal Use Protocols approved through the University of Montana Institutional Animal Care and Use Committee (IACUC).

For some analyses, we used previously generated targeted whole exome data (61.7-Mb spanning 213,164 intervals; ~25-Mb protein-coding exons, ~28-Mb untranslated region, ~9-Mb intronic or intergenic) for 80 snowshoe hares (21× mean coverage) collected from Washington (WA; *n*=13 winter-brown, *n*=13 winter-white), Oregon (OR; *n*=13 winter-brown, *n*=13 winter-white), Montana (MT; *n*=14 winter-white), and southwest British Columbia (BC; *n*=14 winter-brown; Jones et al. 2018). Hares from OR and WA were collected in the Cascade Range where populations are polymorphic for winter coat color (Fig. 1A). Hares from Seeley Lake in western MT are winter-white individuals, while those from BC were collected in low-lying regions near the Pacific coast where snowshoe hares are all winter-brown (Fig. 1A). To infer the history of hybridization, we performed whole genome resequencing of three black-tailed jackrabbits from OR and California (CA) and two winter-brown snowshoe hares from OR and BC. These samples complement WGS data previously generated for two black-tailed jackrabbits from Nevada (NV; one of which was sequenced to higher coverage in this study) and snowshoe hares from MT, WA, Utah (UT), and Pennsylvania (PA; Jones et al. 2018). We extracted genomic DNA following the Qiagen DNeasy Blood and Tissue kit protocol (Qiagen, Valencia, CA) and prepared genomic libraries following the KAPA Hyper prep kit manufacturer's protocol. For all libraries, we sheared genomic DNA using a Covaris E220evolution ultrasonicator and performed a stringent size selection using a custom-prepared carboxyl-coated magnetic bead mix (Rohland

and Reich 2012) to obtain average genomic fragment sizes of 400-500 bp. We determined indexing PCR cycle number for each library with quantitative PCR (qPCR) on a Stratagene Mx3000P thermocycler (Applied Biosystems) using a DyNAmo Flash SYBR Green qPCR kit (Thermo Fisher Scientific). Final libraries were size-selected again with carboxyl-coated magnetic beads, quantified with a Qubit (Thermo Fisher Scientific), and pooled for sequencing by Novogene (Novogene Corporation Ltd.; Davis, CA) on two lanes of Illumina HiSeq4000 using paired-end 150 bp reads.

To resolve the history of selection on the winter-brown *Agouti* allele, we performed targeted enrichment and sequencing to genotype 106 hares at the *Agouti* locus (*n*=37 WA, *n*=64 OR, *n*=5 MT). We developed a custom set of IDT xGen Lockdown probes spanning a 596.4 kb interval centered on the *Agouti* gene and extending to flanking regions (chromosome 4:5,250,800-5,847,200; coordinates based on the European rabbit (*Oryctolagus cuniculus*) oryCun2 genome build). The probe sequences were based on a snowshoe hare pseudoreference genome (~33×; Jones et al. 2018) derived from iterative mapping to the rabbit genome (Carneiro et al. 2014). We targeted 96 uniquely-mapped 100 bp regions (based on low coverage WGS data from Jones et al. (2018)) that contained one or more diagnostic SNPs for winter coat color, allowing us to infer winter coat color for samples based on their *Agouti* genotype. We prepared genomic libraries for targeted *Agouti* sequencing following a modified version of Meyer and Kircher (2010), as described in Jones et al. (2018). We performed hybridization reactions on 500 ng of pooled libraries (10-16 individual libraries per pool), 5 μg of custom prepared snowshoe hare C_0t-1 DNA, and 2 nM of blocking oligos. Washing and recovery of captured DNA was performed following the IDT xGen Lockdown probe hybridization capture protocol (version 2). Each capture library was then amplified in 50 μl reactions with 1X Herculase II reaction buffer,

250 µM each dNTP, 0.5 µM each primer, 1 µl Herculase II fusion polymerase, and 20 µl library template. The PCR temperature profile consisted of a 45 second 98°C denaturation step, followed by 24 cycles of 98°C for 15 seconds, 60°C for 30 seconds, and 72°C for 30 seconds, with a final 72°C elongation step for 1 minute. We cleaned and size-selected final libraries with 1.2X carboxyl-coated magnetic beads and verified target enrichment with qPCR. *Agouti* capture libraries were then pooled and sequenced with other libraries across two lanes of Illumina HiSeq4000 at the University of Oregon Core (Eugene, OR) and Novogene.

Read processing and variant calling

For all raw sequence data, we trimmed adapters and low-quality bases (mean phred-scaled quality score <15 across 4 bp window) and removed reads shorter than 50 base pairs (bp) using Trimmomatic v0.35 (Bolger et al. 2014). We then merged paired-end reads overlapping more than 10 bp and with less than 10% mismatched bases using FLASH2 (Magoč and Salzberg 2011). Cleaned exome and *Agouti* capture reads were mapped using default settings in BWA-MEM v0.7.12 (Li 2013) to the snowshoe hare pseudoreference genome. WGS data were mapped to either the snowshoe hare or a black-tailed jackrabbit pseudoreference, which was also created by iteratively mapping to the rabbit genome (Jones et al. 2018). We used *PicardTools* to remove duplicate reads with the MarkDuplicates function and assigned read group information with the AddOrReplaceReadGroups function. Using GATK v3.4.046 (McKenna et al. 2010), we identified poorly aligned genomic regions with RealignerTargetCreator and performed local realignments with IndelRealigner. We performed population-level multi-sample variant calling using default settings with the GATK UnifiedGenotyper and filtered variants in VCFtools v0.1.14 (Danecek et al. 2011). For whole exome and whole genome data, we filtered genotypes

190 with individual coverage <5× or >70× or with a phred-scaled quality score <30. Additionally, we
191 removed all indel variants and filtered single nucleotide polymorphisms (SNPs) with a phred-
192 scaled quality score <30 and Hardy-Weinberg P<0.001. We required that sites have no missing
193 data across individuals. For targeted *Agouti* SNP data, we additionally filtered heterozygous
194 genotypes with allelic depth ratios >3 and sites with > 50% missing data across individuals. We
195 phased haplotypes and imputed missing data with Beagle v4.1 (Browning and Browning 2007)
196 and used *Haplostrips* (Marnetto and Huerta-Sánchez 2017) to visualize haplotype structure.
197
198 Population size history and inbreeding coefficients of PNW hares
199 We used the program *∂a∂i* (Gutenkunst et al. 2009) to infer historical population size (N)
200 changes in PNW snowshoe hare populations (BC, MT, OR, and WA) using the folded site
201 frequency spectrum (SFS) of synonymous variants from our extensive whole exome data set. We
202 used the folded SFS to be consistent with statistical inferences of the distribution of fitness
203 effects (see below). For each population, we tested a standard neutral equilibrium model, a two-
204 epoch model (single instantaneous N change), a three-epoch model (two instantaneous N
205 changes), an exponential N growth model, and an instantaneous N change + exponential N
206 growth model. We inferred values for parameters ν, the population size relative to ancestral N
207 (N_{anc}; e.g., ν=1 if N=N_{anc}) and t, the time of population size changes in units of $2N_{anc}$
208 generations. We performed 100 independent runs under each model starting with parameter
209 values sampled randomly across a uniform distribution ($0.001<\nu<100$, $0<2N_e t<2$). For each
210 model, we selected parameters with the highest log-likelihood value and chose the overall best
211 model using a composite-likelihood ratio test with the Godambe Information Matrix (Coffman et
212 al. 2016). We further checked the validity of maximum likelihood models by comparing the

predicted SFS to the observed SFS for each population (Fig. S2). We determined 95% confidence intervals for parameter estimates using the Godambe Information Matrix with 100 bootstrap data sets comprised of one randomly selected synonymous SNP per 10 kb.

SFS-based approaches are often underpowered or inappropriate for inferring recent population size changes (Robinson et al. 2014; Beichman et al. 2018). For instance, even with a sufficient sample size, a historically large population that has very recently contracted in size (i.e., not in equilibrium) may nonetheless have a large variance N_e. However, individuals in such populations may exhibit elevated individual inbreeding coefficients (F_{IS}), calculated as $1\text{-}H_o/H_e$ where H_o is the observed heterozygosity and H_e is expected heterozygosity assuming random mating. To examine evidence for recent population contractions, we calculated the mean of the individual inbreeding coefficient (F_{IS}) for each population using VCFtools and tested for significant differences between populations with a two-tailed Student's t-Tests in R (R Core Team 2018).

Mutational load and the distribution of fitness effects

For each PNW population, we measured the proportion of homozygosity across SNPs with predicted phenotypic effects (nonsynonymous and nonsense) as an indicator for relative differences in mutational load under a recessive deleterious mutation model (González-Martínez et al. 2017). We tested for significant differences in the proportion of homozygosity across populations using two-sided Z-tests for proportions in R (R Core Team 2018). Additionally, we used whole exome data to infer the distribution of selection coefficients of segregating variation, more commonly referred to as the distribution of fitness effects (DFE). In principle, we can infer the DFE from the SFS of selected sites because neutral, weakly deleterious, and strongly

236 deleterious variation should segregate at different frequencies in populations (Keightley and
237 Eyre-Walker 2010). The DFE of segregating variation is commonly inferred by first fitting a
238 population history model to the SFS of neutral sites (often synonymous SNPs) and then fitting a
239 mutational model to the SFS of selected sites (often nonsynonymous SNPs), while controlling
240 for the effect of population history (i.e., changes in N) on the SFS of selected sites (Keightley
241 and Eyre-Walker 2010). Here we implement this approach using the *Fit∂a∂i* module (Kim et al.
242 2017). We used the maximum likelihood parameter values from our inferred demographic model
243 to control for population history and fit a simple DFE to the folded SFS of nonsynonymous
244 variants (identified with SNPeff; Cingolani et al. 2012) described by a gamma distribution of
245 selective effects with a shape (α) and scale (β) parameter. To estimate variance in shape and
246 scale parameters, we used 100 bootstrap datasets randomly sampling 50% of nonsynonymous
247 sites and performed 10 independent runs on each dataset. We used random starting values
248 between 0.001 and 1 for the shape parameter and values between 0.01 and 200,000 for the scale
249 parameter. To scale the DFE from relative selection coefficients ($2N_{anc}s$) to absolute selection
250 coefficients (s), we divided the scale parameter by $2N_{anc}$ (Kim et al. 2017).
251
252 <u>The timing of hybridization</u>
253 If hybridization between snowshoe hares and black-tailed jackrabbits is rare, then the age of
254 hybridization may also reflect the age of *Agouti* introgression. We used two complementary
255 approaches to estimate the timing of hybridization between PNW snowshoe hares and black-
256 tailed jackrabbits. Previous phylogenetic analysis of partial cytochrome *b* sequences revealed
257 that some PNW snowshoe hares carry introgressed mitochondrial DNA (mtDNA) genomes
258 derived from hybridization with black-tailed jackrabbits (Cheng et al. 2014; Melo-Ferreira et al.

2014). We estimated the age of mtDNA introgression using complete mtDNA genomes for snowshoe hares (n=56) and black-tailed jackrabbits (n=5) that we assembled *de novo* from newly and previously generated WGS data (Jones et al. 2018) with the program NOVOPlasty (Dierckxsens et al. 2017). We aligned individual mtDNA assemblies, including the rabbit mtDNA reference as an outgroup (total assembled length= 16,251 bp), using default settings in Clustal W v2.1 (Larkin et al. 2007) and visually verified alignment quality. We then estimated a maximum clade credibility tree and node ages with a Calibrated Yule model in BEAST 2 (Bouckaert et al. 2014), assuming a strict molecular clock and an HKY substitution model using empirical base frequencies. We specified default priors for the kappa and gamma shape parameters and used a gamma distribution (alpha=0.001, beta=1000) as a prior for the clock rate and birth rate parameter. We ran the MCMC for 5 million steps and calibrated divergence times using a log-normal distribution for the rabbit-*Lepus* node age with a median of 11.8 million generations (95% prior density: 9.8–14.3; Matthee et al. 2004).

We also examined patterns of autosomal introgression tracts to infer the age of nuclear admixture. Given that mtDNA admixture may have been relatively ancient (Melo-Ferreira et al. 2014), admixture dating approaches based on linkage disequilibrium (LD) may have low power due to erosion of LD through ongoing recombination (Loh et al. 2013). Therefore, we developed an approach to fit the distribution of empirically inferred introgression tract lengths to tract lengths simulated under various models of admixture. We first identified genome-wide tracts of introgression using the program PhylonetHMM (Liu et al. 2014), which assigns one of two parent trees (species tree or hybridization tree) to each variable position using a hidden Markov model. PhylonetHMM robustly distinguishes between incomplete lineage sorting (ILS) and introgression by allowing for switches between gene trees within each parent tree (Liu et al.

2014; Schumer et al. 2016). Alignments of WGS data for the phylogenetic analysis included two black-tailed jackrabbits sampled from CA (BTJR1) and NV (BTJR2), a UT snowshoe hare (previously shown as non-admixed; Jones et al. 2018), and a winter-brown WA snowshoe hare to represent the admixed PNW snowshoe hare population. Here, the species tree is defined as ((WA,UT),(BTJR1, BTJR2)) and the hybridization tree is defined as (UT,(WA,BTJR1/BTJR2)). We specified base frequencies and transmission/transversion rates based on analysis with RAxML. We identified introgression tracts as contiguous regions of the genome with an average hybridization tree probability >95% across 25 variant windows (1 variant step) and excluded introgression tracts shorter than 10-kb (Schumer et al. 2016). We then used the program SELAM (Corbett-Detig and Jones 2016) to simulate a single pulse of admixture (lasting either 1 generation or 100 generations) occurring at a frequency of 0.01%, 0.1%, or 1% and recorded introgression tracts >10kb every 1000 generations for 50,000 generations across 21 autosomes. We performed a goodness of fit test between empirical and simulated tract length distributions using Kolmogorov-Smirnov tests (K-S tests), which measure differences in the cumulative fraction of data across the range of observed values (Massey 1951). To estimate the variance in hybridization timing, we performed K-S tests on 100 bootstrap data sets generated by subsampling 30% of the genome-wide introgression tracts.

The time to most recent common ancestor of the winter-brown haplotype

To understand the history of the spread of winter brown camouflage, we used targeted *Agouti* SNPs to estimate the time to most recent common ancestor (TMRCA) for the winter-brown *Agouti* haplotype in OR (n=47 individuals) and WA (n=35 individuals). We estimated the TMRCA using a Markov chain Monte Carlo approach implemented in *startmrca* (Smith et al.

2018), which leverages information on the length distribution of the fixed selected haplotype and the accumulation of derived mutations. We assumed a constant recombination rate of 1 cM/Mb (Carneiro et al. 2011) and tested an upper and lower estimate for mutation rate in European rabbit (2.02×10^{-9} and 2.35×10^{-9} mutations/site/generation; Carneiro et al. 2012). We also explored the influence of using a divergent population (homozygous winter-white individuals from MT; n=5 individuals) or a local population (homozygous winter-white individuals from OR and WA; n=19 individuals) to represent the ancestral winter-white haplotype (Smith et al. 2018). We assumed chr4:5480355 (in oryCun2 coordinates) as the site of the "selected allele", which lies in the center of the association interval between two strong candidate insertion-deletion mutations in the 5' *cis*-regulatory region of *Agouti* and is perfectly correlated with winter coat color (Jones et al. 2018). We performed 100,000 iterations with a standard deviation of 20 for the proposal distribution and used the final 10,000 iterations to generate posterior TMRCA distributions (Smith et al. 2018).

Simulations of selection on a recessive beneficial allele

Assuming fixation of a single haplotype, the above framework for inferring the TMRCA should reflect the age at which the beneficial haplotype began to increase rapidly in frequency (Smith et al. 2018), which under some conditions may be much more recent than the age of the beneficial mutation itself (Teshima and Przeworski 2006; Kelley 2012). For instance, the masking of recessive alleles to selection at low frequency is expected to decrease the rate at which they begin to increase in frequency, conditional on fixation (Teshima and Przeworski 2006), potentially resulting in a temporal lag between a fixed allele's origin and TMRCA. However, such a scenario may be unlikely as the masking of rare recessive alleles is also expected to

decrease their fixation probability (i.e., 'Haldane's sieve', Haldane 1924; Turner 1981). Alternatively, an environmental change could favor a previously neutral or deleterious variant, resulting in a delayed spread of a segregating mutation. Indeed, Orr and Betancourt (2001) demonstrated that the bias against fixation of recessive alleles disappears when positive selection acts on pre-existing variation in mutation-selection balance. We used simulations to test whether different estimates of the timing of hybridization (i.e., the origin of the winter-brown haplotype) and TMRCA of the winter-brown allele could be due to the masking of recessive alleles at low frequency. Using SLiM 3.1 (Haller and Messer 2019), we simulated an equilibrium population (N_e=257219 for OR population; Table 1) experiencing positive selection on a recessive allele (s=0.026, which reflects our updated median estimate of s for winter-brown haplotype in OR; Jones et al. 2018). At the beginning of the simulations, the recessive allele was introduced at a rate of 0.01% or 0.1% per generation for 1 or 100 generations, which reflects various rates and durations of hybridization. Under each hybridization scenario, we performed 100 simulations and tracked the frequency of the recessive allele every generation, conditioning on fixation. We saved tree sequences (Haller et al. 2019) and analyzed them using *msprime* (Kelleher et al. 2016) to identify the TMCRA for fixed beneficial alleles and determine whether selection resulted in fixation of a single copy (hard sweep) or multiple copies (soft sweep) of the beneficial allele.

Results

Range-edge population history and mutational load

We found support for a single relatively strong N contraction (i.e., a two-epoch model) occurring ~24-100 kya in OR, WA, and BC hares (Table 1, Fig. S2). In contrast, the history of the MT population was characterized by an instantaneous + exponential N change model, in which the

351 population experienced a sudden 17× expansion ~129 kya followed by a gradual reduction to
352 ~53% of N_{anc}. Despite population contractions, estimates of contemporary N_e across all
353 populations were relatively large (161654-257219; Table 1).
354 Using the same exome data set, we previously estimated the joint SFS for pairs of
355 snowshoe hare populations to infer histories of population split times, migration rates, and
356 effective population size in *∂a∂i* (Jones et al. 2018). These pairwise models supported histories
357 of high symmetrical migration rates between populations and *N* contractions following
358 population splits, but generated significantly smaller estimates of contemporary N_e compared to
359 the new estimates that we report in Table 1. However, we made a scaling error while estimating
360 θ (= $4N_e\mu$) under these previous models. This error affected our previously reported
361 demographic parameter estimates for snowshoe hares (Table S9 in Jones et al. 2018) and
362 associated selection coefficient parameter estimates (e.g., previous mean s_{WA}=0.024, s_{OR}=0.015;
363 updated mean s_{WA} =0.049, s_{OR}=0.027; Durrett and Schweinsberg 2005; Jones et al. 2018), but not
364 the main inference of introgression at *Agouti* underlying the genetic basis of polymorphic coat
365 color in snowshoe hares. After scaling parameter values to the correct value of θ and excluding
366 models beyond *a priori* divergence time parameter bounds (>500 thousand years), we found that
367 our maximum likelihood demographic model (reported here in Table S1) still includes high
368 migration rates between populations (~1-2.63 migrants per generation), but with appreciably
369 larger N_e estimates than we previously reported and that are comparable to our new estimates
370 (Table 1).
371 We found significantly elevated F_{IS} in the coastal BC population compared to the other
372 three PNW populations (p<0.01; Fig. 1B), which combined with our previous inference of
373 elevated LD in this population (Jones et al. 2018) could suggest recent inbreeding and population

size reduction. We further found a significantly higher proportion of homozygosity for synonymous, nonsynonymous, and nonsense SNPs in BC relative to other populations (Fig. 1C), which suggests elevated mutational load in BC under a recessive deleterious mutation model. BC individuals also have a significantly higher proportion of strongly deleterious nonsynonymous variants in (27.7%; $|s| \geq 10^{-3}$) relative to other populations (0.8-3.2%; Fig. 1D, Table S2). Because we have the same sample size for MT and BC (n=14 individuals) this striking difference in the DFE is likely not the result of the small BC sample size, which can lead to overestimation of the proportion of strongly deleterious variation (Kim et al. 2017). Notably, if synonymous SNPs used for demographic inference experience direct or linked selection (e.g., Akashi 1994; Stoletzki and Eyre-Walker 2006; Resch et al. 2007; Pouyet et al. 2018), then our demographic model could be misinferred (Ewing and Jensen 2016) in such a way that we will underestimate the strength of purifying selection on non-synonymous SNPs. Regardless, assuming levels of linked selection are similar across populations, the relative differences we observe in the DFE are unlikely driven by weak or linked selection on synonymous variants.

The history of hybridization and introgression

From our complete mtDNA assemblies, we estimated a divergence time of 3.299 million generations ago (95% HPD interval: 2.555-4.255 million generations ago; Fig. 2) between black-tailed jackrabbit and non-introgressed snowshoe hares, which is consistent with previous estimates of species' split times (Matthee et al. 2004; Melo-Ferreira et al. 2014; Jones et al. 2018). Within the non-introgressed snowshoe hare mtDNA clade, we found a relatively deep split between the UT snowshoe hare (representing the 'Rockies' cluster identified by Cheng et al.

2014) and all other snowshoe hares (641 thousand generations ago, 95% HPD interval: 476-834 thousand generations ago; Fig. 2).

A significant portion of snowshoe hares from the PNW (100% of OR hares and 50% of WA hares) formed a reciprocally monophyletic clade relative to black-tailed jackrabbits (100% posterior node support; Fig. 2). As previously demonstrated through coalescent simulations (Melo-Ferreira et al. 2014), this phylogenetic pattern cannot be plausibly explained by ILS and is consistent with asymmetric introgression of black-tailed jackrabbit mtDNA into snowshoe hares. As expected, mtDNA was not associated with winter coat color in the PNW polymorphic zone (chi-squared P=1). However, if we assume that hybridization is rare then mtDNA may track the same hybridization event that introduced winter-brown *Agouti* variation into PNW hares. The estimated split time between black-tailed jackrabbit and introgressed PNW hare mtDNA sequences was 516 thousand generations ago (95% HPD interval: 381-668 thousand generations ago, Fig. 2). However, this split time does not account for segregating ancestral polymorphism (Arbogast et al. 2002) or unsampled mtDNA variation within black-tailed jackrabbits. If we assume extant variation in snowshoe hares represents a single mtDNA introgression event, then the TMRCA of introgressed PNW snowshoe hare variation suggests a more recent date of mtDNA introgression of ~228 thousand generations ago (95% HPD interval: 168-301 thousand generations ago).

Our previous work revealed elevated signatures of genome-wide nuclear admixture presumably coincident with introgression of seasonal camouflage variation (Jones et al. 2018). Here we identified 1878 individual introgression tracts (median length = 28,940 bp), encompassing ~1.99% of the genome (Fig. 3). Across various simulated hybridization scenarios, the most strongly supported age of hybridization was 7-9 thousand generations ago with ranges

of 95% confidence intervals spanning 6-10.5 thousand generations ago (Fig. S4). Different rates of admixture or admixture pulse lengths appeared to have little effect on the inferred hybridization age or the overall fit to empirical data (Fig. S4). Furthermore, we observed poor model fitting for very recent hybridization (< 5 thousand generations ago).

Positive selection for winter-brown camouflage

We identified the *Agouti* region as one of the longest (209,012 bp) and most highly supported introgression tracts (mean introgression probability=0.99) in the WA winter-brown hare (Fig. 4). To understand the history of positive selection on brown winter camouflage, we estimated the TMRCA of the selected winter-brown *Agouti* haplotype in snowshoe hares using targeted sequencing across the *Agouti* region (mean coverage per interval 34× ± 17×). Using a divergent population, a local population, or both to represent the ancestral haplotype had little effect on TMRCA estimates (Table S3), so here we present estimates using both populations. Under a low or high estimate of the rabbit mutation rate, we inferred a TMRCA of approximately 1278 generations (95% CI: 1135-1441 generations) or 1226 generations (95% CI: 1054-1408 generations) for the winter-brown OR haplotype and approximately 1392 generations (95% CI: 1153-1607 generations) or 972 generations (95% CI: 766-1169 generations) for the WA haplotype, respectively (Table S3). We observed no consistent allelic differences between the fixed haplotypes in WA and OR (Fig. 4), consistent with a hard selective sweep.

Haplotype-based methods are known to underestimate the TMRCA and accounting for this systematic error produces TMRCA estimates of approximately 2-4 thousand generations (for a fully recessive allele, $\log_2(\text{estimate/true}) \approx -1.5$; Kelley 2012) for the winter-brown haplotype in OR and WA. If our estimates are accurate, then there appears to be a ~3-8 thousand generation

lag between the origin of the winter-brown haplotype in snowshoe hares (i.e., the inferred hybridization date ~ 7-9 thousand generations ago) and the increase in frequency of the winter-brown haplotype in the PNW from a single copy. Simulations show that such temporal lags are expected for selection on recessive variation, however the duration of this lag (and the total sojourn time) is negatively associated with the hybridization rate and fixation probability, as expected (Table 2). For instance, under the lowest hybridization rate (0.01% for 1 generation) the mean lag time was 2140 generations (95% CI: 101-8322 generation) with only a 0.8% fixation probability and under the highest hybridization rate (0.1% for 100 generations) the mean lag time was only 625 generations but with 100% fixation probability. Conditional on fixation, increased hybridization rates also tended to be more often associated with soft rather than hard sweeps (e.g., 38% hard sweeps for 0.1% hybridization rate for 100 generations versus 98% hard sweeps for 0.01% hybridization rate for 1 generation). However, under intermediate hybridization scenarios (0.1% for 1 generation or 0.01% for 100 generations), we observed relatively long mean lag times (2514 and 1587 generations, respectively) associated with high probabilities of fixation (12% and 79%, respectively), often through hard selective sweeps (81% and 96%; Table 2).

Discussion

Range-edge adaptation may enhance a species' evolutionary resilience to environmental change (Hampe and Petit 2005; Hill et al. 2011), however rigorous population genetic evaluations of predictions for range-edge demography and adaptation are limited (Bridle and Vines 2007). In snowshoe hares, the evolution of brown winter coats in temperate climates along the PNW coast represents the clearest example of local phenotypic adaptation in this wide-ranging species.

Given its direct link to reduced snow cover, the evolution of brown winter camouflage may further foster persistence of snowshoe hares in the face of climate change (Mills et al. 2018). Here we leveraged our understanding of the genetic basis of brown winter camouflage to examine the history of range-edge adaptation, lending insights into the potential for rapid adaptation following environmental change.

Population history and mutational load at the range edge

Populations along range margins are predicted to be small, limiting their ability to adapt to local conditions (although see Moeller et al. 2011; Graignic et al. 2018). Although we cannot assess relative differences in N_e across the entire hare range, we uncovered high N_e estimates across PNW populations (161654-257219; Table 1), despite evidence for strong ancient population size reductions. However, our N_e estimates derive from predictions of genetic drift (i.e., variance N_e) over long evolutionary time scales and may be a weak reflection of current census sizes, especially if local populations experience migration (Wang and Whitlock 2003) or have undergone recent size changes that are undetectable with the SFS (Beichman et al. 2018). We found evidence of significantly higher inbreeding coefficients and mutational load in coastal (BC) populations relative to the inland and montane populations (Fig. 1), signatures that are indicative of a recent population size reduction (Peischl et al. 2013, 2015; Bosshard et al. 2017; Gilbert et al. 2018). Elevated F_{IS} and LD (Fig. S1 in Jones et al. 2018) could instead be related to cryptic population substructure (i.e., the Wahlund effect; Waples 2015). However, we have found no evidence for substructure or admixture in BC that could produce this effect (Jones et al. in prep). Similar signatures of elevated mutational load (e.g., homozygosity for deleterious alleles) have been found in other range-front populations, including the plant *Mercurialis annua*

(González-Martínez et al. 2017) and in human populations that migrated out of Africa (Henn et al. 2016, although see Simons and Sella 2016). Thus, an intriguing potential explanation for these patterns is that they reflect signatures of a founder event associated with a recent range expansion. Moreover, given that we observe these signatures in the coastal winter-brown population, it is possible that this expansion was enabled by the evolution of locally adaptive brown winter camouflage. Winter-white hares experience heavy predation when mismatched (Zimova et al. 2016) and are not known to occur in low-lying coastal regional west of the Cascade Range (Nagorsen 1983; Mills et al. 2018), suggesting that coastal environments with ephemeral snow cover were likely unoccupied prior to local camouflage adaptation.

Long-term persistence of populations under environmental change ultimately requires adaptive evolution and the ability to colonize novel environments. If the colonization of coastal PNW environments by snowshoe hares was enabled by the evolution of brown winter coats, our results underscore that local adaptation to new environments can act as a negative feedback on fitness through the accumulation of deleterious mutations (Pujol and Pannell 2008; Gilbert et al. 2017; González-Martínez et al. 2017; Stewart et al. 2017; Willi et al. 2018). Although the consequences of mutational load for the persistence of PNW hare populations is unclear, high recessive mutational load may compromise the adaptive potential of populations (Assaf et al. 2015; González-Martínez et al. 2017) and increase the probability of extinction in small populations (Mills and Smouse 1994; Frankham 1998). In experiments of isolated *Tribolium* populations, short-term fitness gains via adaptive evolution were entirely lost over longer time periods as a consequence of increasing mutational load, although fitness could be readily restored through admixture (Stewart et al. 2017). In snowshoe hares, the potential fitness costs linked to mutational load may be mitigated by high gene flow between populations (Table S1) or

511 superseded by the enhanced species-level evolutionary resilience afforded by brown-winter
512 camouflage during periods of declining snow cover. Regardless, we suggest that any
513 conservation efforts to promote adaptation to climate change should weigh the potential for
514 enhanced long-term population persistence against the potential short-term fitness costs that may
515 arise through mutational load.
516
517 Hybridization and the origin of the winter-brown allele
518 Hybridization may play an important role shaping adaptation and expansion of range-edge
519 populations (Pfennig et al. 2016), but evidence for this mode of adaptation stems from only a
520 handful of examples (e.g., flies, Lewontin and Birch 1966; mosquitoes, Besansky et al. 2003;
521 sunflowers, Rieseberg et al. 2007). In snowshoe hares, range and niche expansion into mild
522 PNW coastal environments appears to have been enabled by adaptive introgression, although the
523 history of hybridization has remained unclear. We estimated that mtDNA introgression in PNW
524 snowshoe hares occurred ~228 thousand generations ago, which could be interpreted as a
525 conservative upper-bound for the timing of hybridization with black-tailed jackrabbits.
526 Meanwhile, the genome-wide distribution of introgression tract lengths, which should be less
527 sensitive to ILS and population structure within hares (Liu et al. 2014), suggest a much more
528 recent pulse of hybridization ~7-9 thousand generations ago (Fig. 3, Fig. S5). The different
529 genome-wide and mtDNA estimates may also reflect independent pulses of ancient
530 hybridization. Severe systematic overestimation of divergence dates may be common with
531 mtDNA genomes calibrated with a relatively divergent outgroup because of high mutation rates
532 and substitution saturation (Zheng et al. 2011). The divergence dates among major snowshoe
533 hare mtDNA lineages also appear much deeper than our best estimates derived from population

(nuclear) genomic data (~2-3 fold deeper, unpublished data), which suggests that our analyses based on mtDNA likely overestimate the timing of introgression. We assumed a relatively simple molecular clock model and more complicated models (e.g., relaxed clocks) might better account for mutational processes observed in mtDNA genomes. However, it would seem that there would be little insight to be gained by additional modeling here given the myriad of limitations associated with extrapolating population history from a single stochastic realization of the coalescent process (Hudson and Turelli 2003).

Several recent studies have also noted that introgression is positively correlated with local recombination rate (Nachman and Payseur 2012; Janoušek et al. 2015; Schumer et al. 2018; Edelman et al. 2019; Li et al. 2019; Martin et al. 2019), presumable due to the effects of linked selection against deleterious mutations in hybrids. If this relationship generally holds, then it is possible that our dating approach based on the distribution of introgression tract lengths is also upwardly biased. However, contemporary range overlap between snowshoe hares and black-tailed jackrabbits appears restricted to relatively sharp ecological transitions between sage-scrub and montane forests in OR and CA (Fig. 2) and no records exist of putative hybrids, suggesting that contemporary hybridization is likely exceedingly rare or absent and has not resulted in discernable gene flow. Thus, the collective evidence suggests that historical hybridization between snowshoe hares and black-tailed jackrabbits was not more recent than 5 thousand generations ago. Notably, the timing of genome-wide admixture, assuming 1-2 generations per year in hares (Marboutin and Peroux 1995), appears coincident with the retreat of the Cordilleran ice sheet from low-lying coastal habitats in southern BC and northern WA at the end of the last glacial maximum (~18 thousand years ago; Darvill et al. 2018) and thus the opening of suitable habitat for winter-brown snowshoe hares. This period of rapid climatic change resulted in

557 individualistic range shifts for many North American mammal species (Graham 1986),
558 potentially leading to novel community assemblages and thus promoting hybridization events
559 (Swenson and Howard 2005), which could have created conditions favorable to adaptive
560 introgression.
561
562 The spread of winter-brown camouflage and the tempo of local adaptation
563 Although theory predicts adaptation in small range-edge populations may be slow and
564 mutation-limited, hybridization may alleviate the lack of beneficial variation along range
565 margins (Pfennig et al. 2016). Revealing how introgressed alleles adaptively spread through
566 populations is therefore a critical component of understanding the limitations of range-edge
567 adaptation. Here, we identified *Agouti* as one of the largest (>200 kb) and most strongly
568 supported introgression tracts genome-wide (Fig. 4), consistent with our previous study showing
569 exceptionally low genomic divergence in this region between black-tailed jackrabbits and
570 winter-brown snowshoe hares (Jones et al. 2018). Assuming our genome-wide estimates of
571 hybridization age reflect the origination of the *Agouti* allele through introgression (~9 thousand
572 generations ago), our findings suggest a ~3-8 thousand generation delay until the selective sweep
573 of the winter-brown haplotype in the PNW.
574 One potential biological explanation for this temporal lag is that winter-brown
575 camouflage was not immediately beneficial in snowshoe hares. Rather, the winter-brown variant
576 may have initially segregated as a neutral or deleterious allele for a period of time until an
577 environmental shift allowed positive selection to act quickly on standing variation (e.g.,
578 Colosimo et al. 2005). However, our simulations suggest that beneficial recessive alleles
579 segregating at frequencies as high as ~10% (equivalent to simulations of 0.1% hybridization rate

for 100 generations) take on average ~5612 generations (95% CI: 4319-6757 generations) to reach fixation (Table 2). Thus, under an environmental shift scenario, the starting frequency of the winter-brown variant would likely have to be quite large (>10%) in order for selection to quickly drive it to fixation. Although allelic fixation under this model would be virtually guaranteed (Table 2), we suspect that such a high level of hybridization between black-tailed jackrabbits and snowshoe hares is unlikely given their ecological distinctiveness and our lower estimate of the genome-wide proportion of introgression (~1.99%). Furthermore, the high starting allele frequency needed to result in rapid fixation is at odds with the evidence that selection fixed a single haplotype, as higher hybridization rates tended to result in softer sweeps (Table 2).

An alternative explanation for the delayed rise in frequency of the winter-brown allele invokes the limits of positive selection on recessive variation, which is predicted to result in an extended period of drift while at low frequency until homozygous recessive genotypes become more common. Consistent with this, we find significant temporal lags between the timing of hybridization and the TMRCA of fixed beneficial recessive alleles under low and moderate rates of hybridization. Although fixation under our lowest simulated rate of hybridization was highly unlikely (~0.8%; Table 2), the two intermediate scenarios still resulted in relatively high fixation probabilities (12-78%) and tended to produce hard sweeps (81-96%), consistent with observed patterns of genetic variation at the winter-brown *Agouti* haplotype. These results demonstrate that one does not need to invoke changing selective coefficients to explain the apparent lag between the origin and the TMRCA of the winter-brown allele. Rather, our data are consistent with the winter-brown variant being immediately beneficial, although predominately hidden to selection, after introduced through hybridization at moderate frequency (~0.1-1%). Indeed, this

603 mutation-limited scenario is consistent with other known instances of colonization of novel
604 environments through the evolution of locally adaptive camouflage in Nebraska deer mice and
605 White Sands lizards (Laurent et al. 2016; Pfeifer et al. 2018; Harris et al. 2019).

606 Rates of adaptation at range edges are potentially an important component of species'
607 responses to climate change (Hampe and Petit 2005). Our study highlights the key role that
608 hybridization can play in seeding adaptive variation and facilitating range expansion during
609 periods of environmental change. In some cases, introgression appears to facilitate rapid
610 adaptation to environmental change (Norris et al. 2015; Oziolor et al. 2019). However,
611 introgression may not always be an efficient solution for rapid adaptation, as here we
612 demonstrate that the rate of adaptation to novel mild winter environments in snowshoe hares
613 appears to have been limited by the dominance coefficient of the winter-brown allele.
614 Collectively, our findings demonstrate key factors that promote and limit adaptation to changing
615 environments and, in particular, highlight the importance of characterizing genetic dominance of
616 beneficial variants for understanding rates of adaptation and range expansion under climate
617 change.

618

619 ## Acknowledgements

620 We thank E. Cheng and K. Garrison for assistance with sample collection. We thank J. Melo-
621 Ferreira, P. C. Alves, M. S. Ferreira, N. Herrera, E. Kopania, A. Kumar, M. Zimova, K.
622 Garrison, N. Edelman, and the UNVEIL network for helpful discussions. We thank B. Kim for
623 assistance with *Fit∂a∂i* analysis. Funding and support for this research was provided a National
624 Science Foundation (NSF) Graduate Research Fellowship (DGE-1313190), NSF Doctoral
625 Dissertation Improvement Grant (DGE-1702043), NSF Graduate Research Opportunities

626 Worldwide, NSF EPSCoR (OIA-1736249), and NSF (DEB-0841884), the Drollinger-Dial
627 Foundation, American Society of Mammalogists Grant-in-aid of Research, and a Swiss
628 Government Excellence Scholarship. Original sequence data are available in the Sequence Read
629 Archive (www.ncbi.nlm.nih.gov/sra). Previously generated whole exome and genome sequence
630 data of snowshoe hare (BioProject PRJNA420081, SAMN02782769, SAMN07526959) are also
631 available in the Sequence Read Archive.

632

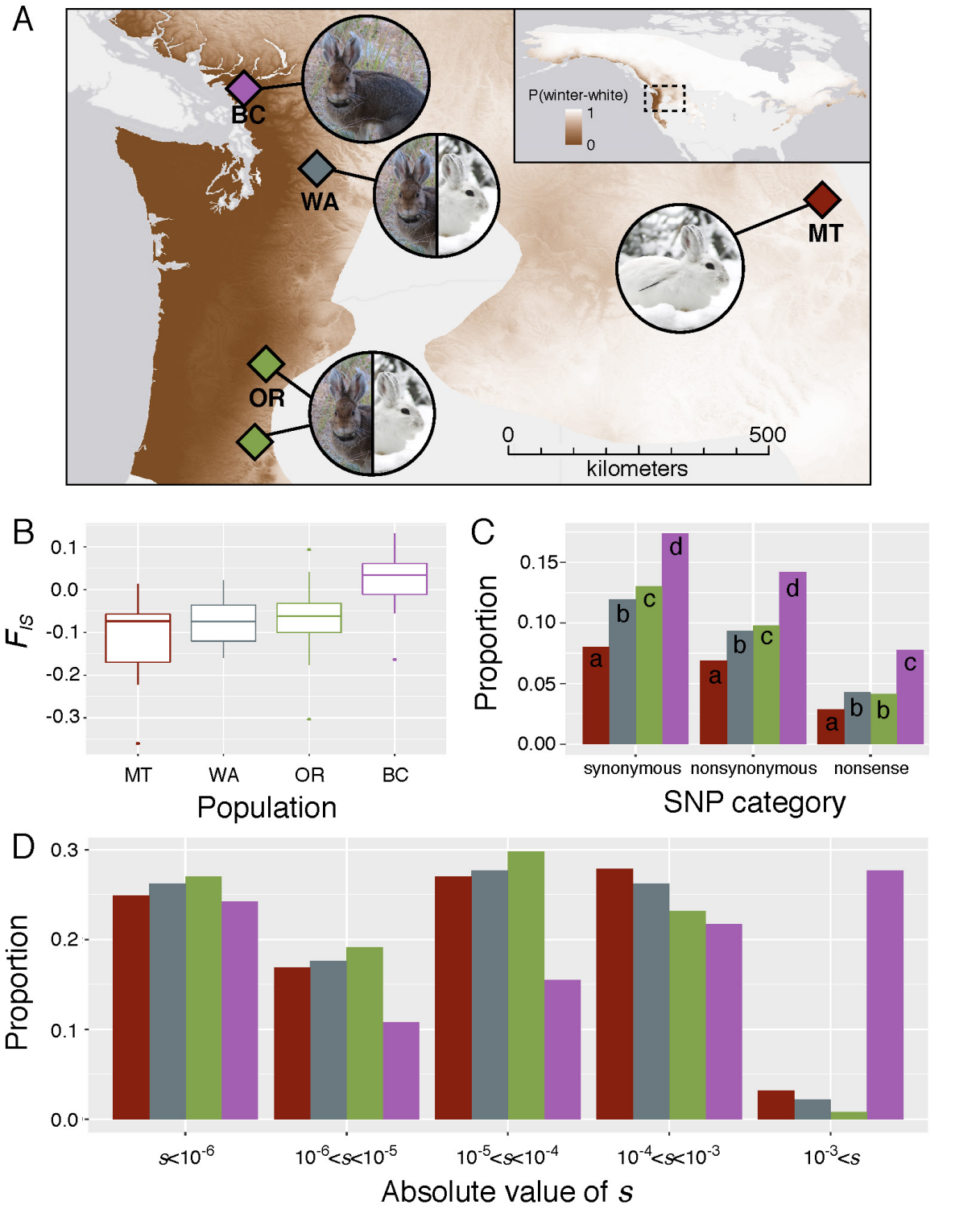

633

634 **Figure 1. (A)** Snowshoe hare range map colored by the probability of winter-white camouflage

635 (white=1, brown=0). The Pacific Northwest region is magnified and shows sampling localities

and coat color phenotypes for BC (purple), MT (red), OR (green), and WA (blue) populations used to generate whole exome data. (**B**) Box-and-whisker plots representing distributions of individual inbreeding coefficients (F_{IS}) within each population. (**C**) The proportion of homozygosity across PNW populations for SNPs classified as synonymous, nonsynonymous (missense), or nonsense. Different letters denote significant differences between populations ($p<0.01$). (**D**) The inferred distribution of fitness effects for each population shown as the proportion of mutations with given selection coefficients.

643

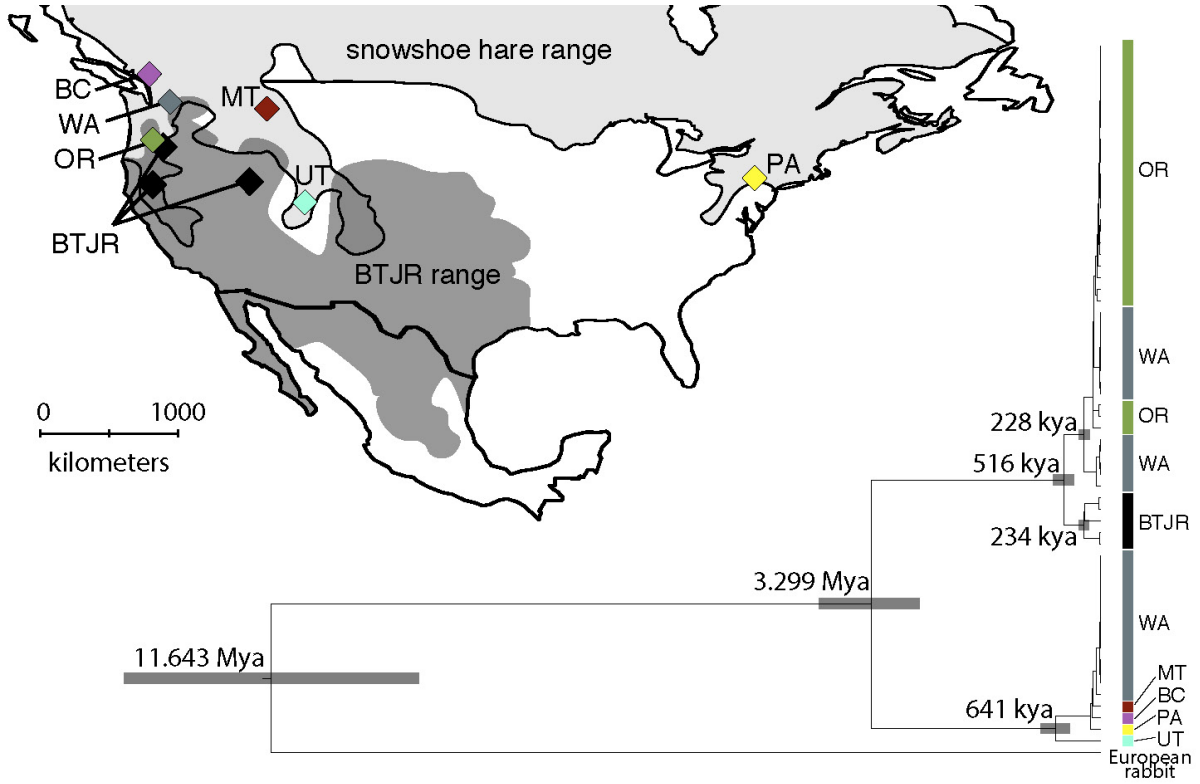

644

645 **Figure 2.** Snowshoe hare and black-tailed jackrabbit (BTJR) ranges with sampling localities for
646 whole genome sequencing. The phylogenetic tree is a maximum clade credibility tree based on
647 whole mitochondrial genome assemblies of snowshoe hares and black-tailed jackrabbits
648 (European rabbit as outgroup) with median estimated split times for crucial nodes. Sample
649 locality names and colors correspond to those on the map. Gray rectangles show the 95% highest
650 posterior density (HPD) for each node age estimate.

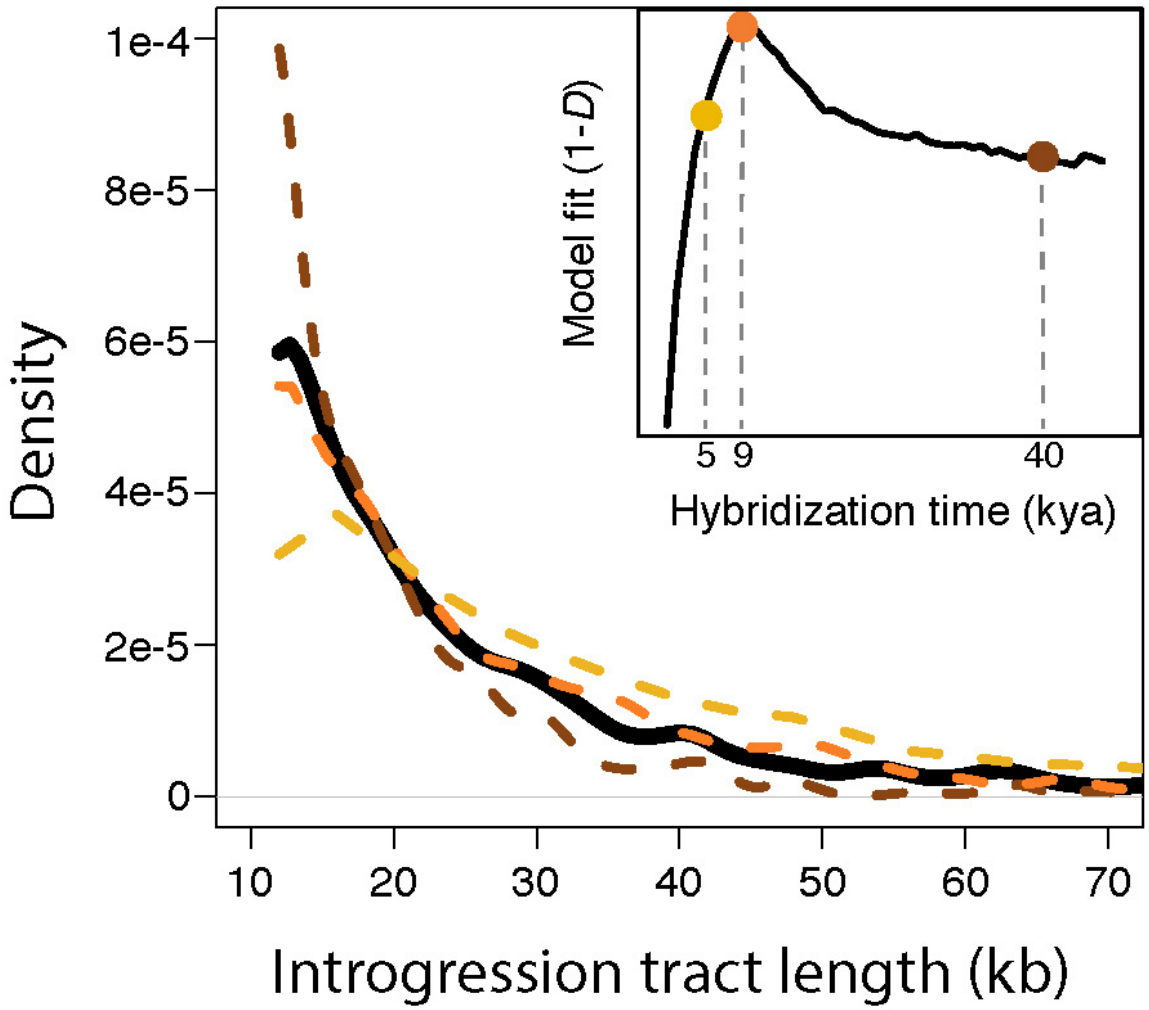

Figure 3. Empirical and simulated distributions of introgression tract lengths. The black line shows the empirical distribution of genome-wide introgression tract lengths in snowshoe hares. Colored dashed lines show simulated tract length distributions at three time points following a 100 generation pulse of hybridization at 0.1% frequency (yellow= 5 kya, orange=9 kya, brown=40 kya). The inset figure shows the overall fit of simulated introgression tract lengths to the empirical distribution through time, with hybridization occurring 9 kya as the model with the strongest fit (95% confidence intervals: 8-10.5 kya).

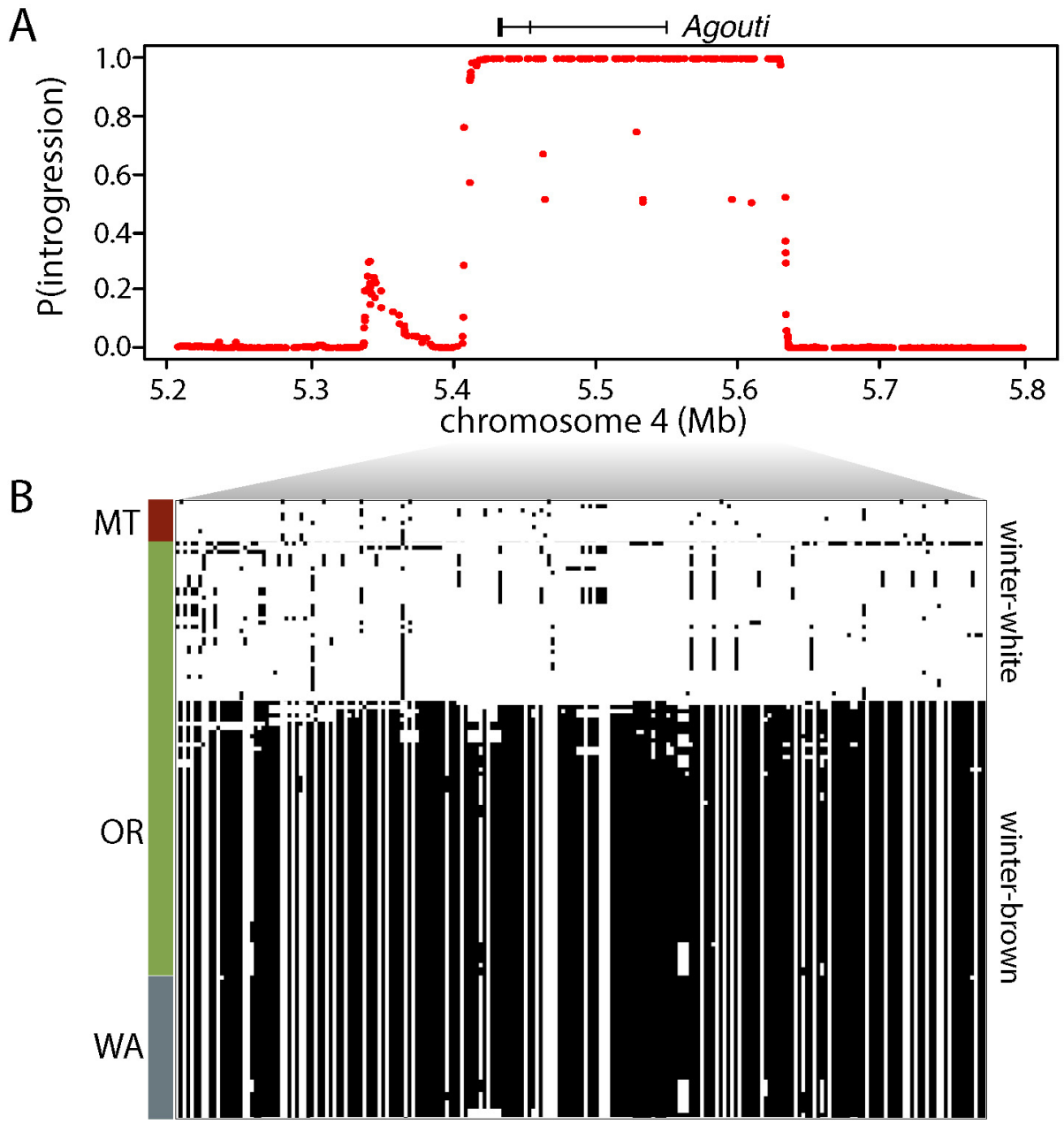

Figure 4. (**A**) Phylonet-HMM classification of the probability of introgression for each variable position across the *Agouti* locus. (**B**) Haplotype structure across the inferred introgressed *Agouti* interval (chr4:5424111-5633123) for winter-white and winter-brown PNW snowshoe hares.

Table 1. Maximum likelihood demographic model parameter estimates.

Population	Model	N_{anc}	N_B	N_F	t (generations)
MT	Inst. change + exp. growth	459809 (450035-469582)	8121810 (5984297-10344665)	245430 (197252-295473)	129400 (98087-161953)
BC	Two-epoch	669265 (662769-675760)	210484 (184353-237086)	-	97853 (70702-125517)
WA	Two-epoch	509979 (503464-516493)	161654 (125444-198747)	-	24357 (20061-28755)
OR	Two-epoch	494903 (482587-507220)	257219 (191394-326076)	-	52540 (44017-61431)

Values in parentheses are the 95% confidence intervals. N_{anc} = population size of common ancestor; N_B = population size following instantaneous change at time t. N_F is the population size following an exponential change beginning immediately after time t.

Table 2. Results from simulations of positive selection on recessive variation.

	1 generation pulse		100 generation pulse	
	0.01%	**0.1%**	**0.01%**	**0.1%**
P(fixation)	0.0082 (0.0068-0.010)	0.12 (0.098-0.13)	0.79 (0.71-0.85)	1.0 (0.96-1.0)
P(hard sweep)	0.98 (0.93-0.99)	0.81 (0.72-0.87)	0.96 (0.90-0.98)	0.38 (0.29-0.48)
T(sojourn)	8911 (5179-16208)	9448 (5626-15746)	6472 (5088-15339)	5612 (4319-6757)
T(lag)	2140 (101-8322)	2514 (97-7740)	1587 (87-7253)	624 (91-1899)

The beneficial variant was introduced through hybridization during a 1 or 100 generation pulse at a rate of 0.01% or 0.1%. Data are shown for the probability of fixation (*P*(fixation)), and, conditional on fixation, the probability of a hard selective sweep(*P*(hard sweep)), the mean sojourn time (*T*(sojourn)), and the mean lag time between a fixed mutation's origin and TMRCA (*T*(lag)). In parentheses are 95% confidence intervals.

675 **References**
676
677 Ackerly, D. D. 2003. Community assembly, niche conservatism, and adaptive evolution in
678 changing environments. International Journal of Plant Sciences 164:S165–S184.
679 Akashi, H. 1994. Synonymous codon usage in *Drosophila melanogaster*: natural selection and
680 translational accuracy. Genetics 136:927–935.
681 Antonovics, J. 1976. The nature of limits to natural selection. Annals of the Missouri Botanical
682 Garden 63:224–247.
683 Arbogast, B. S., S. V. Edwards, J. Wakeley, P. Beerli, and J. B. Slowinski. 2002. Estimating
684 divergence times from molecular data on phylogenetic and population genetic timescales.
685 Annual Review of Ecology and Systematics 33:707–740.
686 Assaf, Z. J., D. A. Petrov, and J. R. Blundell. 2015. Obstruction of adaptation in diploids by
687 recessive, strongly deleterious alleles. Proceedings of the National Academy of Sciences
688 of the United States of America 112:E2658-66.
689 Baker, H. G. 1948. Stages in invasion and replacement demonstrated by species of *Melandrium*.
690 The Journal of Ecology 36:96–119.
691 Barton, N. 2001. Adaptation at the edge of a species' range. Pages 365–392 *in* J. Silvertown and
692 J. Antonovics, eds. Integrating ecology and evolution in a spatial context. Blackwell
693 Science.
694 Behrman, K. D., and M. Kirkpatrick. 2011. Species range expansion by beneficial mutations.
695 Journal of Evolutionary Biology 24:665–675.
696 Beichman, A. C., E. Huerta-Sanchez, and K. E. Lohmueller. 2018. Using genomic data to infer
697 historic population dynamics of nonmodel organisms. Annual Review of Ecology,
698 Evolution, and Systematics 49:433–56.
699 Besansky, N. J., J. Krzywinski, T. Lehmann, F. Simard, M. Kern, O. Mukabayire, D. Fontenille,
700 et al. 2003. Semipermeable species boundaries between *Anopheles gambiae* and
701 *Anopheles arabiensis*: evidence from multilocus DNA sequence variation. Proceedings of
702 the National Academy of Sciences of the United States of America 100:10818–23.
703 Bolger, A. M., M. Lohse, and B. Usadel. 2014. Trimmomatic: a flexible trimmer for Illumina
704 sequence data. Bioinformatics 30:2114–2120.
705 Bontrager, M., and A. L. Angert. 2019. Gene flow improves fitness at a range edge under climate
706 change. Evolution Letters 3:55–68.
707 Bosshard, L., I. Dupanloup, O. Tenaillon, R. Bruggmann, M. Ackermann, S. Peischl, and L.
708 Excoffier. 2017. Accumulation of deleterious mutations during bacterial range
709 expansions. Genetics 207:669–684.
710 Bouckaert, R., J. Heled, D. Kühnert, T. Vaughan, C.-H. Wu, D. Xie, M. A. Suchard, et al. 2014.
711 BEAST 2: a software platform for bayesian evolutionary analysis. PLoS Computational
712 Biology 10:e1003537.
713 Bridle, J. R., and T. H. Vines. 2007. Limits to evolution at range margins: when and why does
714 adaptation fail? Trends in Ecology & Evolution 22:140–147.
715 Browning, S. R., and B. L. Browning. 2007. Rapid and accurate haplotype phasing and missing-
716 data inference for whole-genome association studies by use of localized haplotype
717 clustering. The American Journal of Human Genetics 81:1084–1097.
718 Burke, J. M., and M. L. Arnold. 2001. Genetics and the fitness of hybrids. Annual Review of
719 Genetics 35:31–52.
720 Carneiro, M., S. Afonso, A. Geraldes, H. Garreau, G. Bolet, S. Boucher, A. Tircazes, et al. 2011.

721 The genetic structure of domestic rabbits. Molecular Biology and Evolution 28:1801–
722 1816.
723 Carneiro, M., F. W. Albert, J. Melo-Ferreira, N. Galtier, P. Gayral, J. A. Blanco-Aguiar, R.
724 Villafuerte, et al. 2012. Evidence for widespread positive and purifying selection across
725 the European rabbit (*Oryctolagus cuniculus*) genome. Molecular Biology and Evolution
726 29:1837–1849.
727 Carneiro, M., C.-J. Rubin, F. Di Palma, F. W. Albert, J. Alföldi, A. Martinez Barrio, G. Pielberg,
728 et al. 2014. Rabbit genome analysis reveals a polygenic basis for phenotypic change
729 during domestication. Science 345:1074–1079.
730 Cheng, E., K. E. Hodges, J. Melo-Ferreira, P. C. Alves, and L. S. Mills. 2014. Conservation
731 implications of the evolutionary history and genetic diversity hotspots of the snowshoe
732 hare. Molecular Ecology 23:2929–2942.
733 Cingolani, P., A. Platts, L. L. Wang, M. Coon, T. Nguyen, L. Wang, S. J. Land, et al. 2012. A
734 program for annotating and predicting the effects of single nucleotide polymorphisms,
735 SnpEff: SNPs in the genome of *Drosophila melanogaster* strain w1118; iso-2; iso-3. Fly
736 6:80–92.
737 Coffman, A. J., P. H. Hsieh, S. Gravel, and R. N. Gutenkunst. 2016. Computationally efficient
738 composite likelihood statistics for demographic inference. Molecular Biology and
739 Evolution 33:591–593.
740 Colosimo, P. F., K. E. Hosemann, S. Balabhadra, G. Villarreal, M. Dickson, J. Grimwood, J.
741 Schmutz, et al. 2005. Widespread parallel evolution in sticklebacks by repeated fixation
742 of *Ectodysplasin* alleles. Science 307:1928–1933.
743 Corbett-Detig, R., and M. Jones. 2016. SELAM: simulation of epistasis and local adaptation
744 during admixture with mate choice. Bioinformatics 32:3035–3037.
745 Danecek, P., A. Auton, G. Abecasis, C. A. Albers, E. Banks, M. A. DePristo, R. E. Handsaker, et
746 al. 2011. The variant call format and VCFtools. Bioinformatics 27:2156–2158.
747 Darvill, C. M., B. Menounos, B. M. Goehring, O. B. Lian, and M. W. Caffee. 2018. Retreat of
748 the western Cordilleran Ice Sheet margin during the last deglaciation. Geophysical
749 Research Letters 45:9710–9720.
750 Dierckxsens, N., P. Mardulyn, and G. Smits. 2017. NOVOPlasty: de novo assembly of organelle
751 genomes from whole genome data. Nucleic Acids Research 45:e18.
752 Durrett, R., and J. Schweinsberg. 2005. A coalescent model for the effect of advantageous
753 mutations on the genealogy of a population. Stochastic Processes and their Applications
754 115:1628–1657.
755 Edelman, N. B., P. B. Frandsen, M. Miyagi, B. J. Clavijo, J. Davey, R. Dikow, G. Garcia-
756 Accinelli, et al. 2019. Genomic architecture and introgression shape a butterfly radiation.
757 Science 366:594–599.
758 Ewing, G. B., and J. D. Jensen. 2016. The consequences of not accounting for background
759 selection in demographic inference. Molecular Ecology 25:135–141.
760 Forsman, A. 2016. Is colour polymorphism advantageous to populations and species? Molecular
761 Ecology 25:2693–2698.
762 Frankham, R. 1998. Inbreeding and extinction: island populations. Conservation Biology
763 12:665–675.
764 Garcia-Ramos, G., and M. Kirkpatrick. 1997. Genetic models of adaptation and gene flow in
765 peripheral populations. Evolution 51:21–28.
766 Gigliotti, L. C., D. R. Diefenbach, and M. J. Sheriff. 2017. Geographic variation in winter

767 adaptations of snowshoe hares (*Lepus americanus*). Canadian Journal of Zoology
768 95:539–545.
769 Gilbert, K. J., S. Peischl, and L. Excoffier. 2018. Mutation load dynamics during
770 environmentally-driven range shifts. PLOS Genetics 14:e1007450.
771 Gilbert, K. J., N. P. Sharp, A. L. Angert, G. L. Conte, J. A. Draghi, F. Guillaume, A. L.
772 Hargreaves, et al. 2017. Local adaptation interacts with expansion load during range
773 expansion: maladaptation reduces expansion load. The American Naturalist 189:368–
774 380.
775 Gilbert, K., and M. C. Whitlock. 2016. The genetics of adaptation to discrete heterogeneous
776 environments: frequent mutation or large-effect alleles can allow range expansion.
777 Journal of Evolutionary Biology 30:591–602.
778 González-Martínez, S. C., K. Ridout, and J. R. Pannell. 2017. Range expansion compromises
779 adaptive evolution in an outcrossing plant. Current Biology 27:2544–2551.
780 Graham, R. W. 1986. Response of mammalian communities to environmental changes during the
781 late Quaternary. Pages 300–313 *in* D. J. and C. T. J., eds. Community Ecology. Harper &
782 Row, New York.
783 Graignic, N., F. Tremblay, and Y. Bergeron. 2018. Influence of northern limit range on genetic
784 diversity and structure in a widespread North American tree, sugar maple (*Acer*
785 *saccharum* Marshall). Ecology and Evolution 8:2766–2780.
786 Griffin, P. C., and L. S. Mills. 2009. Sinks without borders: Snowshoe hare dynamics in a
787 complex landscape. Oikos 118:1487–1498.
788 Gutenkunst, R. N., R. D. Hernandez, S. H. Williamson, and C. D. Bustamante. 2009. Inferring
789 the joint demographic history of multiple populations from multidimensional SNP
790 frequency data. PLoS Genetics 5:e1000695.
791 Haldane, J. B. S. 1924. A mathematical theory of natural and artificial selection Part I.
792 Transactions of the Cambridge Philosophical Society 23:19–41.
793 ———. 1930. A mathematical theory of natural and artificial selection (Part VI, Isolation).
794 Mathematical Proceedings of the Cambridge Philosophical Society 26:220–230.
795 Haller, B. C., J. Galloway, J. Kelleher, P. W. Messer, and P. L. Ralph. 2019. Tree-sequence
796 recording in SLiM opens new horizons for forward-time simuilations of whole genomes.
797 Molecular Ecology Resources 19:552–566.
798 Haller, B. C., and P. W. Messer. 2019. SLiM 3: Forward genetic simulations beyond the Wright-
799 Fisher model. Molecular Biology and Evolution 36:632–637.
800 Hampe, A., and R. J. Petit. 2005. Conserving biodiversity under climate change: the rear edge
801 matters. Ecology Letters 8:461–467.
802 Harris, R. B., K. Irwin, M. R. Jones, S. Laurent, R. D. H. Barrett, R. D. H. Nachman, J. M. Good,
803 et al. 2019. The population genetics of crypsis in vertebrates: recent insights from mice,
804 hares, and lizards. Heredity doi:10.1038/s41437-019-0257-4.
805 Hedrick, P. W. 2013. Adaptive introgression in animals: examples and comparison to new
806 mutation and standing variation as sources of adaptive variation. Molecular Ecology
807 22:4606–4618.
808 Henn, B. M., L. R. Botigué, S. Peischl, I. Dupanloup, M. Lipatov, B. K. Maples, A. R. Martin, et
809 al. 2016. Distance from sub-Saharan Africa predicts mutational load in diverse human
810 genomes. Proceedings of the National Academy of Sciences of the United States of
811 America 113:E440-9.
812 Hill, J. K., H. M. Griffiths, and C. D. Thomas. 2011. Climate change and evolutionary

adaptations at species' range margins. Annual Review of Entomology 56:143–159.
Holt, R. D., and R. Gomulkiewicz. 1997. How does immigration influence local adaptation? A reexamination of a familiar paradigm. The American Naturalist 149:563–572.
Hudson, R. R., and M. Turelli. 2003. Stochasticity overrules the "three-times rule": genetic drift, genetic draft, and coalescence times for nuclear loci versus mitochondrial DNA. Evolution 57:182–190.
Huerta-Sánchez, E., X. Jin, Asan, Z. Bianba, B. M. Peter, N. Vinckenbosch, Y. Liang, et al. 2014. Altitude adaptation in Tibetans caused by introgression of Denisovan-like DNA. Nature 512:194–197.
Janoušek, V., P. Munclinger, L. Wang, K. C. Teeter, and P. K. Tucker. 2015. Functional organization of the genome may shape the species boundary in the house mouse. Molecular Biology and Evolution 32:1208–1220.
Jones, M. R., L. S. Mills, P. C. Alves, C. M. Callahan, J. M. Alves, D. J. R. Lafferty, F. M. Jiggins, et al. 2018. Adaptive introgression underlies polymorphic seasonal camouflage in snowshoe hares. Science 360:1355–1358.
Kawecki, T. J. 2008. Adaptation to marginal habitats. Annual Review of Ecology, Evolution, and Systematics 39:321–342.
Keightley, P. D., and A. Eyre-Walker. 2010. What can we learn about the distribution of fitness effects of new mutations from DNA sequence data? Philosophical Transactions of the Royal Society B: Biological Sciences 365:1187–93.
Kelleher, J., A. M. Etheridge, and G. McVean. 2016. Efficient coalescent simulation and genealogical analysis for large sample sizes. PLOS Computational Biology 12:e1004842.
Kelley, J. L. 2012. Systematic underestimation of the age of selected alleles. Frontiers in Genetics 3:165.
Kim, B. Y., C. D. Huber, and K. E. Lohmueller. 2017. Inference of the distribution of selection coefficients for new nonsynonymous mutations using large samples. Genetics 206:345–361.
Kirkpatrick, M., and N. H. Barton. 1997. Evolution of a species' range. The American Naturalist 150:1–23.
Lamichhaney, S., J. Berglund, M. S. Almén, K. Maqbool, M. Grabherr, A. Martinez-Barrio, M. Promerová, et al. 2015. Evolution of Darwin's finches and their beaks revealed by genome sequencing. Nature 518:371–375.
Larkin, M. A., G. Blackshields, N. P. Brown, R. Chenna, P. A. McGettigan, H. McWilliam, F. Valentin, et al. 2007. Clustal W and Clustal X version 2.0. Bioinformatics 23:2947–2948.
Laurent, S., S. P. Pfeifer, M. L. Settles, S. S. Hunter, K. M. Hardwick, L. Ormond, V. C. Sousa, et al. 2016. The population genomics of rapid adaptation: disentangling signatures of selection and demography in white sands lizards. Molecular Ecology 25:306–323.
Lewontin, R. C., and L. C. Birch. 1966. Hybridization as a source of variation for adaptation to new environments. Evolution 20:315–336.
Li, G., H. V Figueiró, E. Eizirik, and W. J. Murphy. 2019. Recombination-aware phylogenomics reveals the structured genomic landscape of hybridizing cat species. Molecular Biology and Evolution 36:2111–2126.
Li, H. 2013. Aligning sequence reads, clone sequences and assembly contigs with BWA-MEM. arXiv 1303.3997.
Liu, K. J., J. Dai, K. Truong, Y. Song, M. H. Kohn, and L. Nakhleh. 2014. An HMM-based comparative genomic framework for detecting introgression in eukaryotes. PLoS

Computational Biology 10:e1003649.
Loh, P.-R., M. Lipson, N. Patterson, P. Moorjani, J. K. Pickrell, D. Reich, and B. Berger. 2013. Inferring admixture histories of human populations using linkage disequilibrium. Genetics 193:1233–1254.
Lynch, M., J. Conery, and R. Burger. 1995. Mutation accumulation and the extinction of small populations. The American Naturalist 146:489–518.
Magoč, T., and S. L. Salzberg. 2011. FLASH: fast length adjustment of short reads to improve genome assemblies. Bioinformatics 27:2957–2963.
Marboutin, E., and R. Peroux. 1995. Survival pattern of European hare in a decreasing population. The Journal of Applied Ecology 32:809–816.
Marnetto, D., and E. Huerta-Sánchez. 2017. Haplostrips: revealing population structure through haplotype visualization. Methods in Ecology and Evolution 8:1389–1392.
Martin, S. H., J. Davey, C. Salazar, and C. Jiggins. 2019. Recombination rate variation shapes barriers to introgression across butterfly genomes. PLoS Biology 17:e2006288.
Massey, F. J. 1951. The Kolmogorov-Smirnov test for goodness of fit. Journal of the American Statistical Association 46:68–78.
Matthee, C. A., B. J. Van Vuuren, D. Bell, and T. J. Robinson. 2004. A molecular supermatrix of the rabbits and hares (Leporidae) allows for the identification of five intercontinental exchanges during the Miocene. Systematic Biology 53:433–447.
McKenna, A., M. Hanna, E. Banks, A. Sivachenko, K. Cibulskis, A. Kernytsky, K. Garimella, et al. 2010. The Genome Analysis Toolkit: A MapReduce framework for analyzing next-generation DNA sequencing data. Genome Research 20:1297–1303.
Melo-Ferreira, J., F. A. Seixas, E. Cheng, L. S. Mills, and P. C. Alves. 2014. The hidden history of the snowshoe hare, *Lepus americanus*: extensive mitochondrial DNA introgression inferred from multilocus genetic variation. Molecular Ecology 23:4617–4630.
Meyer, M., and M. Kircher. 2010. Illumina sequencing library preparation for highly multiplexed target capture and sequencing. Cold Spring Harbor Protocols 5:pdb.prot5448.
Miao, B., Z. Wang, and Y. Li. 2016. Genomic analysis reveals hypoxia adaptation in the Tibetan Mastiff by introgression of the Grey Wolf from the Tibetan Plateau. Molecular Biology and Evolution 34:734–743.
Mills, L. S., E. V Bragina, A. V Kumar, M. Zimova, D. J. R. Lafferty, J. Feltner, B. M. Davis, et al. 2018. Winter color polymorphisms identify global hot spots for evolutionary rescue from climate change. Science 359:1033–1036.
Mills, L. S., and P. E. Smouse. 1994. Demographic consequences of inbreeding in remnant populations. The American Naturalist 144:412–431.
Mills, L. S., M. Zimova, J. Oyler, S. Running, J. T. Abatzoglou, and P. M. Lukacs. 2013. Camouflage mismatch in seasonal coat color due to decreased snow duration. Proceedings of the National Academy of Sciences of the United States of America 110:7360–7365.
Moeller, D. A., M. A. Geber, and P. Tiffin. 2011. Population genetics and the evolution of geographic range limits in an annual plant. The American Naturalist 178:S44-61.
Nachman, M. W., and B. A. Payseur. 2012. Recombination rate variation and speciation: theoretical predictions and empirical results from rabbits and mice. Philosophical Transactions of the Royal Society B: Biological Sciences 367:409–421.
Nagorsen, D. W. 1983. Winter pelage colour in snowshoe hares (*Lepus americanus*) from the Pacific Northwest. Canadian Journal of Zoology 61:2313–2318.

905 Nelson, T. C., M. R. Jones, J. P. Velotta, A. S. Dhawanjewar, and R. M. Schweizer. 2019.
906 UNVEILing connections between genotype, phenotype, and fitness in natural
907 populations. Molecular Ecology 28:1866–1876.
908 Norris, L. C., B. J. Main, Y. Lee, T. C. Collier, A. Fofana, A. J. Cornel, and G. C. Lanzaro. 2015.
909 Adaptive introgression in an African malaria mosquito coincident with the increased
910 usage of insecticide-treated bed nets. Proceedings of the National Academy of Sciences
911 of the United States of America 112:815–20.
912 Orr, H. A., and A. J. Betancourt. 2001. Haldane's sieve and adaptation from the standing genetic
913 variation. Genetics 157:875–884.
914 Oziolor, E. M., N. M. Reid, S. Yair, K. M. Lee, S. Guberman VerPloeg, P. C. Bruns, J. R. Shaw,
915 et al. 2019. Adaptive introgression enables evolutionary rescue from extreme
916 environmental pollution. Science 364:455–457.
917 Pardo-Diaz, C., C. Salazar, S. W. Baxter, C. Merot, W. Figueiredo-Ready, M. Joron, W. O.
918 McMillan, et al. 2012. Adaptive introgression across species boundaries in *Heliconius*
919 butterflies. PLoS Genetics 8:e1002752.
920 Peischl, S., I. Dupanloup, M. Kirkpatrick, and L. Excoffier. 2013. On the accumulation of
921 deleterious mutations during range expansions. Molecular Ecology 22:5972–5982.
922 Peischl, S., M. Kirkpatrick, and L. Excoffier. 2015. Expansion load and the evolutionary
923 dynamics of a species range. The American Naturalist 185:E81–E93.
924 Pfeifer, S. P., S. Laurent, V. C. Sousa, C. R. Linnen, M. Foll, L. Excoffier, H. E. Hoekstra, et al.
925 2018. The evolutionary history of Nebraska deer mice: local adaptation in the face of
926 strong gene flow. Molecular Biology and Evolution 35:792–806.
927 Pfennig, K. S., A. L. Kelly, and A. A. Pierce. 2016. Hybridization as a facilitator of species range
928 expansion. Proceedings of the Royal Society B: Biological Sciences 283:20161329.
929 Polechová, J. 2018. Is the sky the limit? On the expansion threshold of a species' range. PLoS
930 Biology 16:e2005372.
931 Pouyet, F., S. Aeschbacher, A. Thiéry, and L. Excoffier. 2018. Background selection and biased
932 gene conversion affect more than 95% of the human genome and bias demographic
933 inferences. eLife 7:e36317.
934 Pujol, B., and J. R. Pannell. 2008. Reduced responses to selection after species range expansion.
935 Science 321:96.
936 R Core Team. 2018. R: A language and environment for statistical computing. R Foundation for
937 Statistical Computing, Vienna, Austria.
938 Resch, A. M., L. Carmel, L. Mariño-Ramírez, A. Y. Ogurtsov, S. A. Shabalina, I. B. Rogozin,
939 and E. V. Koonin. 2007. Widespread positive selection in synonymous sites of
940 mammalian genes. Molecular Biology and Evolution 24:1821–1831.
941 Rieseberg, L. H., S.-C. Kim, R. A. Randell, K. D. Whitney, B. L. Gross, C. Lexer, and K. Clay.
942 2007. Hybridization and the colonization of novel habitats by annual sunflowers.
943 Genetica 129:149–165.
944 Robinson, J. D., A. J. Coffman, M. J. Hickerson, and R. N. Gutenkunst. 2014. Sampling
945 strategies for frequency spectrum-based population genomic inference. BMC
946 Evolutionary Biology 14:254.
947 Rohland, N., and D. Reich. 2012. Cost-effective, high-throughput DNA sequencing libraries for
948 multiplexed target capture. Genome Research 22:939–946.
949 Schumer, M., R. Cui, D. L. Powell, G. G. Rosenthal, and P. Andolfatto. 2016. Ancient
950 hybridization and genomic stabilization in a swordtail fish. Molecular Ecology 25:2661–

951 2679.
952 Schumer, M., C. Xu, D. L. Powell, A. Durvasula, L. Skov, C. Holland, J. C. Blazier, et al. 2018.
953 Natural selection interacts with recombination to shape the evolution of hybrid genomes.
954 Science 360:656–660.
955 Sgrò, C. M., A. J. Lowe, and A. A. Hoffmann. 2011. Building evolutionary resilience for
956 conserving biodiversity under climate change. Evolutionary Applications 4:326–337.
957 Simons, Y. B., and G. Sella. 2016. The impact of recent population history on the deleterious
958 mutation load in humans and close evolutionary relatives. Current Opinion in Genetics &
959 Development 41:150–158.
960 Slatyer, R. A., M. Hirst, and J. P. Sexton. 2013. Niche breadth predicts geographical range size: a
961 general ecological pattern. Ecology Letters 16:1104–1114.
962 Smith, J., G. Coop, M. Stephens, and J. Novembre. 2018. Estimating time to the common
963 ancestor for a beneficial allele. Molecular Biology and Evolution 35:1003–1017.
964 Song, Y., S. Endepols, N. Klemann, D. Richter, F.-R. Matuschka, C.-H. Shih, M. W. Nachman,
965 et al. 2011. Adaptive introgression of anticoagulant rodent poison resistance by
966 hybridization between old world mice. Current Biology 21:1296–1301.
967 Stewart, G. S., M. R. Morris, A. B. Genis, M. Szűcs, B. A. Melbourne, S. J. Tavener, and R. A.
968 Hufbauer. 2017. The power of evolutionary rescue is constrained by genetic load.
969 Evolutionary Applications 10:731–741.
970 Stoletzki, N., and A. Eyre-Walker. 2006. Synonymous codon usage in *Escherichia coli*: selection
971 for translational accuracy. Molecular Biology and Evolution 24:374–381.
972 Swenson, N. G., and D. J. Howard. 2005. Clustering of contact zones, hybrid zones, and
973 phylogeographic breaks in North America. The American Naturalist 166:581–591.
974 Taylor, S. A., and E. L. Larson. 2019. Insights from genomes into the evolutionary importance
975 and prevalence of hybridization in nature. Nature Ecology and Evolution. Nature
976 Publishing Group.
977 Teshima, K. M., and M. Przeworski. 2006. Directional positive selection on an allele of arbitrary
978 dominance. Genetics 172:713–8.
979 Turner, J. R. G. 1981. Adaptation and evolution in *Heliconius*: a defense of NeoDarwinism.
980 Annual Review of Ecology and Systematics 12:99–121.
981 Wang, J., and M. C. Whitlock. 2003. Estimating effective population size and migration rates
982 from genetic samples over space and time. Genetics 163:429–446.
983 Waples, R. S. 2015. Testing for Hardy-Weinberg proportions: have we lost the plot? Journal of
984 Heredity 106:1–19.
985 Willi, Y., M. Fracassetti, S. Zoller, and J. Van Buskirk. 2018. Accumulation of mutational load
986 at the edges of a species range. Molecular Biology and Evolution 35:781–791.
987 Wright, S. 1931. Evolution in Mendelian populations. Genetics 16:97–159.
988 Zheng, Y., R. Peng, M. Kuro-o, and X. Zeng. 2011. Exploring patterns and extent of bias in
989 estimating divergence time from mitochondrial DNA sequence data in a particular
990 lineage: a case study of salamanders (Order Caudata). Molecular Biology and Evolution.
991 Narnia.
992 Zimova, M., L. S. Mills, and J. J. Nowak. 2016. High fitness costs of climate change-induced
993 camouflage mismatch. Ecology Letters 19:299–307.
994